

Introducing PASAVI and PANDVI Methods for Sugarcane Physiological Date Estimation, Using ASTER Images

M. R. Mobasheri^{1*}, M. Chahardoli², and M. Farajzadeh³

ABSTRACT

Ecological studies based on field data have shown that vegetation phenology follows a relatively well-defined temporal pattern. This pattern, that is reflecting the cumulative temperature from the date of the beginning of the growth, can be represented by the use of a suitable model. Due to the spatial, temporal, and ecological complexity of these processes a simple method to monitor phenological behavior of the vegetation canopies through remote sensing has proven elusive. Employing ASTER images from different seasons, might make it possible to produce an algorithm for sugarcane phenological date estimation and as well to monitor different stages of the plant growth from cultivation to harvest. For this, a parameter, namely Physiological Date is employed. Based on the field collected data and selected ASTER Images, 133 Regions Of Interest (ROI) having different Phenological Dates (PD) in units of Degree-Days (DDs) were supplied. One hundred of these samples were taken for modeling and another 33 for testing the models. Such indices as NDVI and SAVI along with PDs for the ROIs were calculated. The correlation between these indices and PDs was investigated. This ended up with the introduction of two models of PANDVI and PASAVI respectively based on the use of NDVI and SAVI indices for PD assessment. PANDVI model showed a better correlation with the field recorded data although either of the models can be well enough predictive.

Keywords: ASTER, Phenology, Remote sensing, Sugarcane.

INTRODUCTION

Monitoring and understanding plant phenology, namely the timing of recurrent biological events, are gaining importance in the context of agricultural studies. Because of the long-term interest of biologists in phenology, many long time series of *in situ* phenological records exist (e.g., from meteorological stations or from "phenological gardens").

However, continuous observations of phenology needed for the study of the effects of environmental parameters on plant phenology in vast vegetated areas, are time

consuming and costly. Consequently, such observations have been derived from remote sensing data (Mobasheri *et al.*, 2007a; Tucker *et al.*, 2001). Various algorithms have so far been applied to derive phenological dates in many studies (Alesheikh and Sadeghi, 2007; Duchemin *et al.*, 2006; Justice *et al.*, 1985; Kang *et al.*, 2003; Lu Deke *et al.*, 1996; Sakamoto *et al.*, 2005; Vin~A *et al.*, 2004; White *et al.*, 2002; Zhanga *et al.*, 2003).

On the other hand, monitoring seasonal changes in vegetation activity and crop phenology over wide areas is essential for many applications such as estimation of net

¹ Remote Sensing Engineering Department, Khajeh Nasir-o-din Toosi University of Technology, Tehran, Islamic Republic of Iran.

² Islamic Azad University, Malayer Branch, Islamic Republic of Iran.

³ Department of Remote Sensing and GIS, Tarbiat Modares University, Tehran, Islamic Republic of Iran.

* Corresponding author; e-mail: mobasheri@kntu.ac.ir



primary production (Kimball *et al.*, 2004; Mobasheri *et al.*, 2007b), and supporting decisions concerning water supply (Digkuhn and Gal, 1996; Mobasheri *et al.*, 2007b). Because of the synoptic coverage and repeated temporal sampling that the satellite observations afford, remotely sensed data may have significant potential for monitoring vegetation phenology at regional to global scales (Myneni *et al.*, 1997). A number of different methods have so far been developed to determine the growing stages of vegetation green up and senescence (start and end up of the growing period). Most of these methods are using time series of Normalized Difference Vegetation Index (NDVI) and/or Soil Adjusted Vegetation Index (SAVI) data from low resolution sensors such as the Advanced Very High Resolution Radiometer (AVHRR) (Kaduk and Heimann, 1996; Lloyd, 1990; White *et al.*, 2002). These indices are based on the red-edge reflectance of the vegetation (ρ_{RED} and ρ_{NIR}) and can be calculated through the following equations:

$$NDVI = \frac{\rho_{NIR} - \rho_{RED}}{\rho_{NIR} + \rho_{RED}} \quad (1)$$

$$SAVI = \frac{(\rho_{NIR} - \rho_{RED})(1 + L)}{\rho_{NIR} + \rho_{RED} + L} \quad (2)$$

Factor L is a constant added to NDVI to increase the contrast between soil and vegetation. Different values are suggested for this factor (Mobasheri, 2006). Until recently, AVHRR products were the only source of global data for this purpose. However, beside poor resolution, the AVHRR was never designed for land applications, so its collection of data cannot be well suited for vegetation monitoring applications. Specifically, the lack of precise calibration, poor geometric registration, and difficulties involved in cloud screening in AVHRR data may result in high levels of noises (Goward *et al.*, 1991; Mobasheri and Sadeghi, 2008).

This shortcoming may be overcome using Terra platform with a valuable ASTER

sensor onboard. In this paper, the first attempt to study sugarcane phenology using data produced through this sensor is presented.

Sugarcane crop with scientific name of *Saccharum*, belongs to the genus *Saccharum* L., of the tribe Andropogoneae in the grass family Poaceae, and is a tall growing cash crop cultivated in the tropical and subtropical regions of the world for its ability to store high concentrations of sucrose in its internodes of the stem. Sugarcane is propagated vegetatively. Its germination refers to the initiation of growth from buds present on the planted setts or on the stems of the stools that remain in the soil after harvest of the previous crop (Qotb, 1963). Setts are normally planted within a few days after the previous harvest to achieve quick crop successions. Buds will germinate within two weeks after planting. Sugarcane grows perennially and the root system, known as ratoon, which remains in the ground, will resprout from each stalk, and consequently ratoon crops normally grow faster than the newly planted crops (Qotb, 1963). Sugarcane growth rate slows down with its sucrose content increasing just around 120 days following planting.

Normally sugarcane will be ready for harvest 12 to 18 months after planting, the harvested part being the sugarcane stalks. Crop phenological stages identified through ASTER data may enable one to estimate crop growth under various regional weather conditions. As an instance, cool winters could be named which result in delayed heading and thus decreased sugarcane yields. Ecological studies, based on field data, have demonstrated that the vegetation phenology follows relatively well-defined temporal patterns. For instance, in deciduous vegetation as well as in many other crops, leaf emergence usually follows a period of rapid growth, and is then followed by a relatively stable period of maximum leaf area. This pattern reflects the cumulative temperature (i.e. simply the number of days) from the date of the beginning of growth, which can be represented through a suitable

model (Villegas *et al.*, 2001). The transition to senescence and dormancy follows a similar, but reverse pattern.

Due to the spatial, temporal, and ecological complexity of these processes some vegetation types exhibit multiple modes of growth and senescence within a single annual cycle. Thus a simple method of monitoring them through remote sensing has proven elusive.

Suitable spatial and spectral resolution and low price make ASTER images one of the best sensors available for agricultural studies. Using different ASTER images from different seasons, it is tried to produce an algorithm for sugarcane phenological date estimation and as well to monitor the different stages of the plant growth from cultivation to harvest.

Many efforts have so far been made for crop yield estimation through a relationship between temperature and yield. Aceituno (1979) suggested a temperature above the growing threshold since no considerable growth occurs at lower temperatures. He used a parameter named Physiological Date (PD) in units of Degree-Days (DDs) for sugarcane. By this, for a day during which the maximum temperature is one degree higher than the growing threshold, the DD is one and if this continues for 30 days then the DDs would be 30 and so on.

The growing rate of many creatures is being controlled through temperature. Vegetation and cold blooded animals need a certain amount of heat energy to move from one stage of their growth to the other in their lifecycles (Aceituno, 1979).

Usually to determine the growing stage of vegetation or insects, their physiological dates will be used (Aceituno, 1979). This parameter is cumulative with its estimation depending on the definition of a growing threshold temperature (related to a certain stage of the creature's) and as well on its increasing rate with temperature.

In this work, the annual cycle of sugarcane phenology inferred from remote sensing is characterized by six transition stages which define the key phenological phases of

sugarcane dynamics at annual time scales. These transition stages are: (1) green up, that is the date of onset of photosynthetic activity during the first month; (2) second growing stage around two months after cultivation; (3) around 4 months after cultivation; (4) after 6 months; (5) after 10 months and (6) after one year of cultivation.

Here, we present a new method, which fits satellite data to an acceptable precision. Based on this method, any transition stage can be identified. To carry out this research, field data collected by sugarcane industry's experts on a routine basis as well as ASTER images are employed.

Site Selection and Data Collection

The study area is a part of Amirkabir and Dea'bal-Khazaie Sugarcane sites located in the north-west of Persian Gulf some 25 kilometers south of Ahvaz in Khuzestan Province, Iran. The location of the field in the UTM system is in zone 39, from 237,361 m to 239,506 m in length and from 3,427,183 m to 3,428,158 m in width (Figure 1). The reason for this selection was the availability of field data, required in this research, in the above-mentioned sites. The selected field is a part of Amir Kabir Sugarcane unit itself a part of 84,000 hectares of sugarcane plantation and industries in Khuzestan Province, north-west of Persian Gulf, Iran.

The required Level1-B Terra/ASTER images in bands 2 and 3N from 2003 to 2006 which covered different sugarcane growing seasons were supplied. To ensure the quality of satellite images, analysis of the weather condition was carried out. Moreover, Subsets of satellite images for different periods of time were produced. Satellite images were corrected for Khuzestan atmosphere using weather data and orbital parameters. Also geometrical correction was made by rotating the image by an angle given in the image header. Maps of 1:25000 were used in the images' geo-referencing control process.

**Table 1.** ASTER image characteristics.

| Image No. | Acquisition date | Image identification code |
|-----------|------------------|--|
| 1 | 2003/06/16 | AST_L1B_00306162003073319_07102003114537_1141.hdf |
| 2 | 2004/06/09 | AST_L1B_00306092004073913_20060626115152_14532.hdf |
| 3 | 2004/7/20 | AST_L1B_00307202004073252_20060626115353_16264.hdf |
| 4 | 2004/7/27 | AST_L1B_00307272004073900_20060626115433_16698.hdf |
| 5 | 2004/08/05 | AST_L1B_00308052004073244_20060626115613_17945.hdf |
| 6 | 2004/09/06 | AST_L1B_00309062004073228_20060626115623_18052.hdf |
| 7 | 2005/04/05 | AST_L1B_00305042005073244_20060626120236_20765.hdf |
| 8 | 2005/09/09 | AST_L1B_00309092005073210_20060626124111_6041.hdf |
| 9 | 2006/04/28 | AST_L1B_00304282006073845_20060626124952_9255.hdf |

Some 20 frames of ASTER images were screened out of which 9 frames of the region in the study area were selected. The particulars of these images are shown in Table 1.

The supplied images are standard products of Level-1B. The images were corrected for the atmospheric effects using ATCOR-2 program. In addition, input data for this program were altitude from sea level, pixel size, date and time of image acquisition, calibration file, such weather parameters as humidity and visibility, sun azimuth, latitude and longitude.

Two bands of red and near-IR were employed in the research (Table 2). The conversion equation used for converting DN values to radiance was [Aster User Handbook Version 2]:

$$\text{Radiance } (\text{Wm}^{-2} \text{ sr}^{-1} \mu\text{m}^{-1}) = (\text{DN} - 1) \times \text{Conversion Coefficient} \quad (3)$$

Conversion coefficients are presented in Table 2.

Table 2. Conversion coefficients for ASTER bands 2 and 3 .

| Band No. | Conversion coefficients | | | Band width μm |
|----------|-------------------------|-------------|-----------|--------------------------|
| | High gain | Normal gain | Low gain1 | |
| 2 | 0.1087 | 0.2174 | 0.290 | 0.63-0.69 |
| 3N | 0.423 | 0.867 | 1.15 | 0.78-0.86 |

METHODOLOGY

Selection of ROI

Regarding the number of images and the number of fields with different physiological dates, and considering the collected data in those fields, 133 ROI samples covering different growing stages were selected. These samples were used for supplying NDVI and SAVI indices. Since it is tried to select samples from the regions with healthy plants and canopies (no stresses and diseases), it is expected to have model outputs close to the field calculated values. The reason for excluding stressed and diseased samples was to find the model for healthy vegetations. Of course after running this model for unknown vegetated areas and comparing the model output (PDs) with those of logbooks, one can recognize if the vegetations are under any kind of stress or diseases. To keep the selected samples free from the effects of the nearby roads, a 50 meter margin from the transportation roads was taken into account. The selected samples are shown in Figure 1.

Preparation of Ground Truth PDs

There are different methods of PD estimation such as Rectangular Method,



Figure 1. Location of the study area (Left), Sampling area (Right).

Triangular Method and Sinusoidal Methods (Aceituno, 1979) among which Rectangular Method is used by (Mobasheri *et al.*, 2008). According to this method the PDs in units of Degree-Days (DDs) can be calculated through equation (4) below

$$PD = \frac{T_{MAX} + T_{MIN}}{2} - T_{THR} \quad (DD) \quad (4)$$

where T_{MAX} and T_{MIN} are maximum and minimum daily temperatures respectively, collected at the nearby weather station on a routine basis and T_{THR} is the threshold temperature that can differ from one plant to the other. This for sugarcane is taken as 16°C (Qotb, 1963).

Using the field supplied vector and the cultivation tables for years 2003 to 2006, the physiological dates for each of the selected ROIs were calculated. The method used was the rectangular method. The input data to the method were cultivation date, image date, maximum and minimum temperatures and the threshold temperature of 16°C for sugarcane as suggested by (Qotb, 1963).

Model Preparation

At this stage, NDVI and SAVI for the selected ROIs were calculated. A value of 0.5 for the soil adjusting factor L was used as suggested by (Allen *et al.*, 2002) although

a value of 0.1 for this factor is suggested by (Mobasheri, 2006) for this region.

To prepare a model for estimation of sugarcane PDs, the calculated NDVI (SAVI) were plotted against phenological dates of 100 ROI samples supplied in the previous stage. The other 33 ROIs will be used for testing the models. Here the averaged NDVIs (SAVIs) were taken as the dependant variables. To select the best index for the assessment of PDs, a regression between NDVI (SAVI) and ground truth PDs was set up.

In calculation of these two indices, samples from the same ROIs were used. This might increase the accuracy in the selection of the best index. The results of the calculations are shown in Table 3.

The temporal profiles of NDVI and SAVI indices are shown in Figures 2 and 3 respectively. As is evident, both indices have approached a constant value in the final growing stages.

That is, with increase in the physiological dates of the crop, the values of NDVI and SAVI saturate and approaching constant figures. From now on, to distinguish between these two approaches, the first one will be called Physiological Age vs. NDVI (PANDVI) while the second one named Physiological Age vs. SAVI (PASAVI).



Table 3. Eextracted NDVI and SAVI indices for selected ROIs from ASTER images.

| ROI No. | PDs (Degree-Days) | Average NDVI | Average SAVI | ROI No. | PDs (Degree-Days) | Average NDVI | Average SAVI | ROI No. | PDs (Degree-Days) | Average NDVI | Average SAVI |
|---------|----------------------|-----------------|-----------------|---------|----------------------|-----------------|-----------------|---------|----------------------|-----------------|-----------------|
| 1 | 2385 | 0.517 | 0.775 | 46 | 1790 | 0.49 | 0.734 | 91 | 3353.75 | 0.701 | 0.973 |
| 2 | 2127.75 | 0.377 | 0.565 | 47 | 1780 | 0.617 | 0.925 | 92 | 3325.5 | 0.691 | 1.036 |
| 3 | 1640 | 0.334 | 0.501 | 48 | 4540 | 0.834 | 1.396 | 93 | 3325.5 | 0.715 | 1.071 |
| 4 | 2150 | 0.469 | 0.551 | 49 | 1048 | 0.139 | 0.208 | 94 | 1374 | 0.273 | 0.41 |
| 5 | 1492.45 | 0.515 | 0.773 | 50 | 2472.55 | 0.791 | 1.104 | 95 | 1050 | 0.229 | 0.037 |
| 6 | 1982 | 0.411 | 0.476 | 51 | 1280 | 0.168 | 0.252 | 96 | 837 | 0.024 | 0.175 |
| 7 | 1900 | 0.338 | 0.506 | 52 | 1921 | 0.563 | 0.844 | 97 | 4197.65 | 0.835 | 1.342 |
| 8 | 1674 | 0.236 | 0.354 | 53 | 4036.4 | 0.762 | 1.143 | 98 | 3520 | 0.817 | 1.251 |
| 9 | 3000 | 0.61 | 0.864 | 54 | 3394.4 | 0.754 | 1.13 | 99 | 2367 | 0.667 | 1.212 |
| 10 | 1407.05 | 0.345 | 0.517 | 55 | 2923 | 0.66 | 0.989 | 100 | 2910 | 0.735 | 1.224 |
| 11 | 1630 | 0.302 | 0.452 | 56 | 1850 | 0.519 | 0.777 | 101 | 3109.45 | 0.655 | 1.04 |
| 12 | 2650 | 0.546 | 0.74 | 57 | 2190 | 0.666 | 0.998 | 102 | 3745.35 | 0.832 | 1.253 |
| 13 | 2520 | 0.542 | 0.692 | 58 | 2301.85 | 0.701 | 1.051 | 103 | 3420 | 0.885 | 1.365 |
| 14 | 2140 | 0.467 | 0.7 | 59 | 2301.85 | 0.724 | 1.085 | 104 | 916 | 0.016 | 0.023 |
| 15 | 1250.65 | 0.237 | 0.518 | 60 | 960 | 0.015 | 0.023 | 105 | 1260 | 0.16 | 0.133 |
| 16 | 1330.25 | 0.358 | 0.537 | 61 | 2494.55 | 0.625 | 0.937 | 106 | 1110 | 0.143 | 0.214 |
| 17 | 643 | 0.045 | 0.429 | 62 | 4430 | 0.84 | 1.365 | 107 | 1154 | 0.063 | 0.094 |
| 18 | 3940 | 0.89 | 1.303 | 63 | 1322 | 0.336 | 0.21 | 108 | 3600 | 0.705 | 1.057 |
| 19 | 2467 | 0.658 | 1.112 | 64 | 2476 | 0.71 | 1.065 | 109 | 4265.4 | 0.89 | 1.278 |
| 20 | 1570 | 0.52 | 0.86 | 65 | 4260 | 0.885 | 1.389 | 110 | 3270 | 0.707 | 1.059 |
| 21 | 1426.35 | 0.413 | 0.78 | 66 | 1230 | 0.21 | 0.079 | 111 | 2749 | 0.728 | 1.091 |
| 22 | 1426.35 | 0.366 | 0.549 | 67 | 1050 | 0.084 | 0.126 | 112 | 3020 | 0.777 | 1.164 |
| 23 | 1255.15 | 0.302 | 0.453 | 68 | 3750 | 0.854 | 1.279 | 113 | 2310 | 0.687 | 1.029 |
| 24 | 2220 | 0.64 | 0.972 | 69 | 1639 | 0.381 | 0.571 | 114 | 4370.9 | 0.825 | 1.17 |
| 25 | 1216 | 0.432 | 0.647 | 70 | 2000 | 0.635 | 0.952 | 115 | 2610 | 0.534 | 0.8 |

Continued...

Table3. Eextracted NDVI and SAVI indices for selected ROIs from ASTER images. (Continued)

| ROI No. | PDs (Degree-Days) | Average NDVI | Average SAVI | ROI No. | PDs (Degree-Days) | Average NDVI | Average SAVI | ROI No. | PDs (Degree-Days) | Average NDVI | Average SAVI |
|---------|----------------------|-----------------|-----------------|---------|----------------------|-----------------|-----------------|---------|----------------------|-----------------|-----------------|
| 26 | 2982.65 | 0.727 | 1.089 | 71 | 4400.3 | 0.795 | 1.151 | 116 | 2860 | 0.751 | 1.177 |
| 27 | 2123 | 0.644 | 0.965 | 72 | 3758.3 | 0.88 | 1.308 | 117 | 2390 | 0.56 | 0.708 |
| 28 | 590 | 0.052 | 0.319 | 73 | 2200 | 0.669 | 1.003 | 118 | 3090 | 0.721 | 1.081 |
| 29 | 978 | 0.103 | 0.155 | 74 | 2694 | 0.738 | 1.106 | 119 | 2238 | 0.627 | 1.099 |
| 30 | 608 | 0.04 | 0.136 | 75 | 2665.75 | 0.71 | 1.223 | 120 | 3356 | 0.724 | 1.085 |
| 31 | 1533 | 0.469 | 0.849 | 76 | 3520 | 0.845 | 1.267 | 121 | 960 | 0.069 | 0.103 |
| 32 | 793 | 0.019 | 0.315 | 77 | 1600 | 0.401 | 0.738 | 122 | 718 | 0.043 | 0.065 |
| 33 | 775 | 0.236 | 0.354 | 78 | 1757.25 | 0.345 | 0.37 | 123 | 661.5 | 0.013 | 0.236 |
| 34 | 750 | 0.026 | 0.039 | 79 | 2828 | 0.557 | 0.767 | 124 | 699.8 | 0.04 | 0.022 |
| 35 | 3714.95 | 0.744 | 1.115 | 80 | 4370 | 0.76 | 1.076 | 125 | 590 | 0.077 | 0.215 |
| 36 | 3714.95 | 0.664 | 0.996 | 81 | 2060 | 0.421 | 0.631 | 126 | 1040 | 0.201 | 0.302 |
| 37 | 830 | 0.08 | 0.321 | 82 | 2870 | 0.779 | 1.168 | 127 | 1740 | 0.48 | 0.446 |
| 38 | 2130.65 | 0.603 | 0.903 | 83 | 3780 | 0.845 | 1.311 | 128 | 712.1 | 0.115 | 0.172 |
| 39 | 3520 | 0.832 | 1.379 | 84 | 1651.9 | 0.258 | 0.386 | 129 | 1800 | 0.288 | 0.28 |
| 40 | 3138.4 | 0.679 | 1.017 | 85 | 2250 | 0.625 | 0.936 | 130 | 952 | 0.351 | 0.526 |
| 41 | 2696 | 0.77 | 1.154 | 86 | 1320 | 0.307 | 0.46 | 131 | 1660 | 0.318 | 0.477 |
| 42 | 2205.75 | 0.667 | 0.999 | 87 | 3496.2 | 0.705 | 1.057 | 132 | 1110 | 0.159 | 0.238 |
| 43 | 3858.15 | 0.695 | 1.042 | 88 | 5060.05 | 0.907 | 1.303 | 133 | 784 | 0.23 | 0.345 |
| 44 | 3069 | 0.721 | 1.08 | 89 | 4418.05 | 0.8 | 1.119 | | | | |
| 45 | 1200 | 0.28 | 0.088 | 90 | 2570 | 0.595 | 0.892 | | | | |

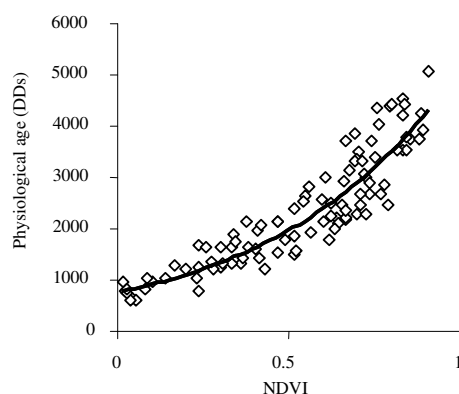


Figure 2. Variation of sugarcane physiological age with the NDVI index for 100 ROI samples (PANDVI model).

These are shown in Figures 3 and 4 for PANDVI and PASAVI respectively. The best fit to these data were curves of the exponential forms. As for PANDVI model the fitted equation was of the form:

$$DD = 755.24e^{1.9204 \cdot NDVI}, R^2 = 0.8745 \quad (5)$$

This for PASAVI was of the form:

$$DD = 804.41e^{1.1879 \cdot SAVI}, R^2 = 0.7754 \quad (6)$$

DISCUSSION

To assess the workability of the PANDVI and PASAVI models, the last 33 ROI

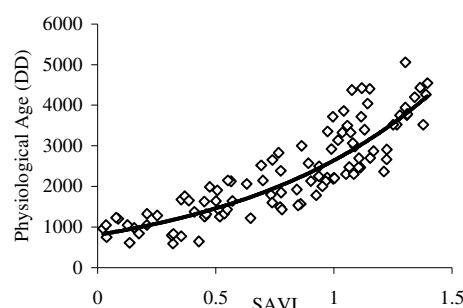


Figure 3. Variation of sugarcane physiological age with the SAVI index for 100 ROI samples (PASAVI model).

samples from Table 3 were used. That is, the predicted PDs by PANDVI and PASAVI models were plotted against field calculated PD values. The results are shown in Figures 4 and 5 respectively. It is found that the RMSE for PANDVI model is 60 (DDs) while for PASAVI it is of the order of 77 (DDs). As can be seen in Figure 4, the distribution of data around bisector is much better than Figure 5 where it is believed that the former is mostly due to the ambiguities related to the soil factor (L) determination in SAVI index.

Also the R^2 of the fitted line for the PANDVI is of the order of 0.9116 while this for PASAVI is 0.8578. However both models can estimate the PDs to an

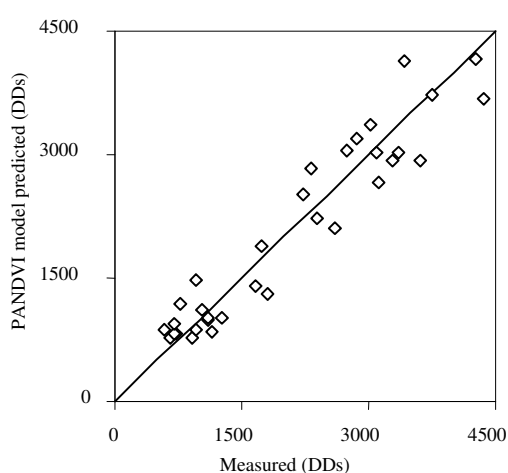


Figure 4. Predicted PDs by PANDVI model against field calculated data.

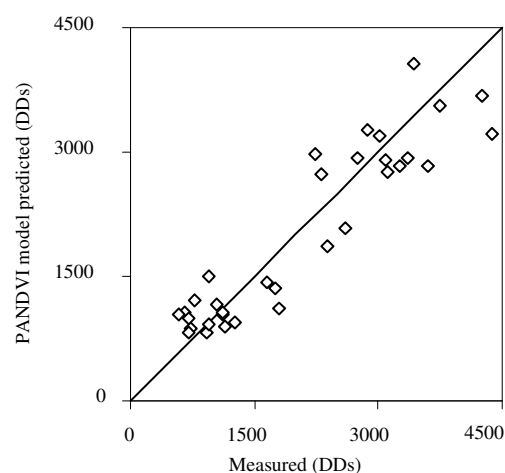


Figure 5. Predicted PDs by PASAVI model against field calculated data.

acceptable level of accuracy. To increase the applicability of these models, it is suggested that: (1) geo-referencing of the images be done as accurate as possible, (2) masking all non vegetated areas by preferably using land cover maps, and (3) correcting the images for the atmospheric effects using local synoptic meteorological parameters as inputs to the atmospheric correction modules.

As an illustration, the PASAVI model has been applied to an ASTER image (Figure 6-a) where the output is a classified image shown in (Figure 6-b). Different classes are defined in Table 4.

Table 4. Classification codes with respect to SAVI and PD values.

| Class | Vegetation cover (%) | SAVI Index | Phenological date (DDs) |
|-------|----------------------|-------------|-------------------------|
| A | 0 | Negative | 0 |
| B | >22 | 0-0.255 | 0-960 |
| C | 23-37 | 0.255-0.450 | 960-1630 |
| D | 38-52 | 0.450-0.675 | 1630-2300 |
| E | 53-65 | 0.675-0.900 | 2300-2980 |
| F | 66-80 | 0.900-1.125 | 2980-3650 |
| G | 81-93 | 1.125-1.306 | 3650-4350 |
| H | 94-100 | 1.306-1.500 | >4350 |



Figure 6-a. ASTER image (RGB-321) used for classification with PASAVI.

CONCLUSIONS

Ecological studies based on field data have demonstrated that the vegetation phenology follows a relatively well-defined temporal pattern. This pattern reflects the cumulative temperature from the beginning date of growth, which can be represented by using a suitable model.

Due to the spatial, temporal, and ecological complexity of the growth processes (some vegetation types exhibit multiple modes of growth and senescence within a single annual cycle), simple methods of monitoring them through remote sensing have proven rather elusive.

Suitable spatial-spectral resolution and low price makes ASTER images one of the most suitable tools for agricultural studies. By using different ASTER images related different seasons, it is possible to produce an algorithm for sugarcane phenological date estimation as well as to monitor different stages of the plant growth from cultivation to harvest. For this purpose a parameter named Physiological Date is employed. Six different growing stages were introduced in the present work. These transitional stages were: (1) green up, the date of onset of photosynthetic activity during the first month; (2) second growing stage around two months after cultivation; (3) around 4 months following cultivation; (4) six months following cultivation; (5) after 10 months and (6) one year past cultivation. In this

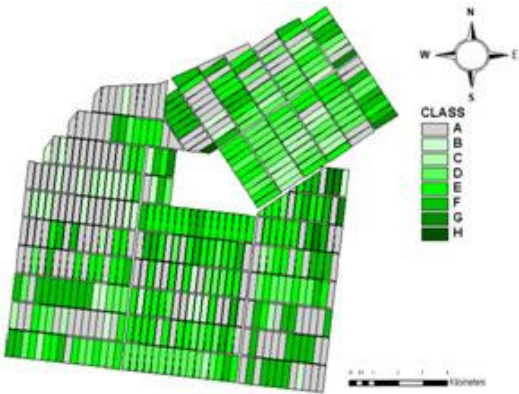


Figure 6-b. Classified image using PASAVI model and Table 4.



work a new method that fits satellite data to an acceptable precision is introduced. Based on this method, any transitional stage can be identified. To implement this research, field data collected by sugarcane industry's experts on a routine basis together with ASTER images were employed.

One hundred and thirty three ROI samples covering different growing stages were selected. These samples were used for supplying NDVI and SAVI indices. Using the field supplied vectors and the cultivation tables for the years 2003 to 2006, the physiological dates for each of the selected ROIs were calculated. To prepare a model for estimation of sugarcane PDs, the calculated NDVI (SAVI) were plotted against phenological dates of 100 ROI samples. The other 33 ROIs were used for testing the models. These models are called PANDVI and PASAVI for NDVI and SAVI respectively. It is found that the RMSE for PANDVI model is 60 (DDs), whereas for PASAVI model it is of the order of 77 (DDs). Also the R^2 of the fitted line for the PANDVI is of the order of 0.91 while this for PASAVI amounts to 0.86.

REFERENCES

1. Aceituno, P. 1979. Statistical Formulator Estimate Heating or Cooling Degree-day, *Agr. Met.*, **20**: 227-232.
2. Alesheikh, A. A. and Sadeghi Naeeni Fard, F. 2007. Design and Implementation of a Knowledge Based System to Improve Maximum Likelihood Classification Accuracy. *Can. J. Remote Sens.*, **33(6)**: 459-467.
3. Allen, R., Waters, R., Tasumi, M., Trezza, R. and Bastianssen, W. 2002. *SEBAL, Surface Energy Balance Algorithms for Land*. Version 1.0, Advanced Training and Users Manual, Idaho Implementation.
4. Digkuhn, M. and Gal, P. 1996. Effect of Drainage Date on Yield and Dry Matter Partitioning in Irrigated Rice. *Field Crops Res.*, **46**: 117-126.
5. Duchemin, B., Hadria, R., Erraki, S., Boulet, G., Maisongrande, P., Chehbouni, A., Escadafal, R., Ezzahar, J., Hoedjes, J. C. B., Kharrou, M. H., Khabba, S., Mougenot B., Oliso, A., Rodriguez, J.-C. and Simonneaux, V. 2006. Monitoring Wheat Phenology and Irrigation in Central Morocco: On the Use of Relationships between Evapo-transpiration, Crops Coefficients, Leaf Area Index and Remotely-sensed Vegetation Indices. *Agric. Water Manage.*, **79**: 1-27.
6. Goward, S. N., Markham, B., Dye, D. G., Dulaney, W. and Yang, A. J. 1991. Normalized Difference Vegetation Index Measurements from the Advanced Very High Resolution Radiometer. *Remote Sens. Environ.*, **35**: 257-277.
7. Justice, C. O., Townshend, J. R. G., Holben, B. N. and Tucker, C. J. 1985. Analysis of the Phenology of Global Vegetation Using Meteorological Satellite Data. *Int. J. Remote Sens.*, **6**: 1271-1318.
8. Kaduk, J. and Heimann, M. 1996. A Prognostic Phenology Model for Global Terrestrial Carbon Cycle Models. *Clim. Res.*, **6**: 1-19.
9. Kang, S. R., Steven, W. and Lim, J. H. 2003. A Regional Phenology Model for Detection Onset of Greenness in Temperate Mixed Forests: An Application of MODIS Leaf Area. *Remote Sens. Environ.*, **86**: 232-242.
10. Kimball, J., McDonald, K., Running, S. and Frolking, S. 2004. Satellite Radar Remote Sensing of Seasonal Growing Seasons for Boreal and Subalpine Evergreen Forests. *Remote Sens. Environ.*, **90**: 243-258.
11. Lloyd, D. 1990. A Phenological Classification of Terrestrial Vegetation Cover Using Shortwave Vegetation Index Imagery. *Int. J. Remote Sens.*, **11**: 2269-2279.
12. Lu'Deke, M. K. B., Ramge, P. H. and Kolhmaier, G. H. 1996. The Use of Satellite NDVI Data for the Validation of Global Vegetation Phenology Models: Application to the Frankfurt Biosphere Model. *Ecol. Modell.*, **91**: 255-270.
13. Mobasheri, M. R. 2006. Producing Evapo-Transpiration Map for Khuzestan Province, South West of Iran. A Project Report Funded by KWEO. (In Farsi)
14. Mobasheri, M. R., Rezaie, Y. and Valadan-Zouje, M. J. 2007a. A Method in Extracting Vegetation Quality Parameters Using Hyperion Images, with Application to Precision Farming. *World Appl. Sci. J.*, **2(5)**: 476-483.

15. Mobasheri, M. R., Jokar, J., Ziaeiian, P. and Chahardoli, M. 2007b. On the Methods of Sugarcane Water Stress Detection Using Terra/ASTER Images. *American-Eurasian J. Agric. Environ. Sci.*, **2(3)**: 619-627.
16. Mobasheri, M. R. and Sadeghi Naeini, A. 2008. Using IRS Products to Recover 7ETM⁺ Defective Images. *Am. J. Appl. Sci.*, **5(6)**: 618-625.
17. Myneni, R. B., Keeling, C. D., Tucker, C. J., Asrar, G. and Nemani, R. R. 1997. Increased Plant Growth in the Northern High Latitudes from 1981 to 1991. *Nat.*, **386**: 698–702.
18. Qotb, E. 1963. Parameters Influencing Sugarcane Phenology and Related Problems in Khuzestan. Tehran University Press (Farsi Ed.), PP. 51-58.
19. Sakamoto, T., Yokozawa, M., Toritani, H., Shibayama, M., Ishitsuka, N. and Ohno, H. 2005. A Crop Phenology Detection Method Using Time-series MODIS Data. *Remote Sens. Environ.*, **96**: 366–374.
20. Tucker, C. J., Slayback, D. A., Pinzon, J. E., Los, S. O., Myneni, R. B. and Taylor, M. G. 2001. Higher Northern Latitude Normalized Difference Vegetation Index and Growing Season Trends from 1982 to 1999. *Int. J. Biometeorol.*, **45**: 184–190.
21. Villegas, D., Aparicio, N., Blanco, R. and Royo, C. 2001. Biomass Accumulation and Main Stem Elongation of Durum Wheat Grown under Mediterranean Conditions. *Ann. Bot.*, **88**: 617–627.
22. Vin[^]A, A., Gitelson, A. A., Rundquist, D. C., Keydan, G., Leavitt, B. and Schepers J. 2004. Monitoring Maize (*Zea mays* L.) Phenology with Remote Sensing. *Agron. J.* **96**: 1139–1147.
23. White, M. A., Nemani, R. R., Thornton, P. E. and Running, S. W. 2002. Satellite Evidence of Phenological Differences between Urbanized and Rural Areas of the Eastern United States Deciduous Broadleaf Forest. *Ecosyst.*, **5**: 260–277.
24. Zhanga, X., Friedla, M. A., Schaaf, C. B., Strahler, A. H., Hodges, J. C. F., Gaoa, F., Reed, B. C. and Huetec, A. 2003. Monitoring Vegetation Phenology Using MODIS. *Remote Sens. Environ.*, **84**: 471–475.

ارائه دو روش PASAVI و PANDVI برای تخمین سن فیزیولوژیکی گیاه نیشکر با استفاده از تصاویر ASTER

م. ر. مبشری، م. چهاردولی و م. فرج زاده

چکیده

مطالعات اکولوژیکی مبتنی بر داده‌های میدانی نشان داده‌اند که فنولوژی گیاهان از الگوهای زمانی که بخوبی تعریف شده باشند پیروی می‌کنند. این الگوها منعکس کننده اثر تجمعی دما از زمان شروع رشد گیاه می‌باشند و می‌توانند با مدل‌های مناسبی تعریف شوند. بعلا پیچیدگی این فرآیندها ناشی از قدرت تفکیک فضایی، قدرت تفکیک زمانی و اکولوژیکی، همواره از ارائه یک مدل ساده برای پایش فنولوژی گیاه با استفاده از سنجش از دور، پرهیز شده‌است. با استفاده از تصاویر ASTER از فصول مختلف، این امکان وجود دارد که بتوان الگوریتمی برای تخمین رفتار فنولوژیکی خیمه‌های گیاهی و پایش مراحل مختلف رشد گیاه از لحظه کاشت تا برداشت ارائه نمود. برای اینکار از پارامتری بنام سن فیزیولوژیکی استفاده شده‌است. بر اساس داده‌های میدانی جمع‌آوری شده و تصاویر ASTER مناسب، ۱۳۳ ناحیه (ROI)



در مزارع نیشکر با سن‌های فیزیولوژیکی (PD) متفاوت برحسب (درجه-روز) انتخاب گردید. ۱۰۰ مورد از این داده‌ها برای تولید الگوریتم و ۳۳ مورد بقیه برای آزمون مورد استفاده قرار گرفت. شاخص‌های گیاهی همچون NDVI و SAVI به‌مراه PD برای این ROI ها محاسبه گردید. آنگاه همبستگی بین این شاخص‌ها و PD ها مورد بررسی قرار گرفت. این بررسی منجر به تولید دو الگوریتم بنامهای PANDVI و PASAVI بترتیب مبتنی بر استفاده از شاخص‌های NDVI و SAVI گردید. نتایج نشان داد که PANDVI همبستگی بیشتری با داده‌های میدانی دارد گرچه عملکرد هر دو مدل به اندازه کافی رضایت‌بخش بوده-است.